Thermoluminescence Properties for X-ray of Cr-doped Al_2O_3 Ceramics

Kiyomitsu Shinsho,[1*] Daiki Maruyama,[1] Shin Yanagisawa,[1] Yusuke Koba,[2]
Mizuki Kakuta,[1] Kazuki Matsumoto,[3] Hiroaki Ushiba,[3] and Takayuki Andoh[4]

[1]Tokyo Metropolitan University, 7-2-10 Higashi-Oku, Arakawa-ku, Tokyo 116-8551, Japan
[2]QST NIRS, 4-9-1 Anagawa, Inage-ku, Chiba-shi, Chiba 263-8555, Japan
[3]Chiyoda Technol Corporation, 1-7-12 Yushima, Bunkyo-ku, Tokyo 113-8681, Japan
[4]Chibaceramic MFG Co. Ltd., 2-10-14 Inage-higashi, Inage-ku, Chiba-shi, Chiba 263-0031, Japan

We investigated the basic thermoluminescence (TL) characteristics of Cr-doped low-melting-point Al_2O_3. The concentration of Cr_2O_3 in this study ranged from 0.01 to 1.0 wt%. Owing to the stabilization of the trapped state caused by Cr doping, we successfully improved the low-melting-point Al_2O_3 fading property dramatically. Then, the sensitivity of 0.05 wt% Cr-doped Al_2O_3 to X-rays was about 4.8 times higher than that of the nondoped Al_2O_3, allowing the Al_2O_3 to maintain its attractive properties to X-rays. Furthermore, the 0.05 wt% Cr-doped Al_2O_3 had good properties for dosimetry owing to its high TL sensitivity, high reproducibility, high radiation resistivity, and high thermal stability in two dimensions. Finally, we demonstrated two-dimensional (2D) verifications of radiotherapy (RT) plans using Cr-doped Al_2O_3 ceramic plates. The results had good agreement with RT plans.

1. Introduction

Modern radiotherapy (RT) can focus radiation into a tumor with high precision, which leads to better therapeutic gains over other methods. Therefore, both the irradiation field and the dosage require highly precise validation. Currently, a radiochromic film is typically used for the two-dimensional (2D) verification of RT plans. It has good tissue equivalence and a high spatial resolution. However, the technique has some limitations, including high material costs in certain countries and a narrow dynamic range, among others. There are some alternatives to the use of the radiochromic film. The thermoluminescence dosimeter (TLD) is one of the alternatives. Recently, with the advent of the CCD camera, the high-resolution imaging of large areas has become much faster, so the amount of research on X-ray imaging using 2D-TLD was increased.[1–6] In particular, human-tissue-equivalent 2D-TLD has been paid more attention owing to focusing needs in the medical field. However, it has low reproducibility, low signal-to-noise ratio, and low solidity; thus, there is no suitable human-tissue-equivalent 2D-TLD.

High-purity Al_2O_3 has been reported to maintain high sensitivity, but it is not a suitable material for 2D-TLD owing to its high melting point of 2,072 °C.[7] Thus, the costs of both the material and its production have become high. We focused on a thermoluminescence (TL) phosphor Al_2O_3 with a low melting point of approximately 1600 °C with some sintering assistance. It is easy to produce a large plate using Al_2O_3, owing to the low costs of the materials and production system, compared with that in the case of the high-purity Al_2O_3. We reported that a commercially available Al_2O_3 plate with a low melting point of 1600 °C has a low material cost and a wide dynamic range, and is reusable.[8] However, it is necessary to improve this material's fading property, owing to an unstable trap state at a glow peak temperature of 148 °C. In this study, we investigated the basic TL characteristics of Cr-doped low-melting-point Al_2O_3 for improving the TL properties. The Cr_2O_3 concentration in this study ranged from 0.01 to 1.0 wt%. The 0.05 wt% Cr-doped Al_2O_3 ceramic yielded the best results. Finally, we demonstrated the verification of the RT plan with 0.05 wt% Cr-doped Al_2O_3 ceramic plates.

2. Materials and Methods

2.1 Materials and glow curve measurement system

The low-melting-point Al_2O_3 of Chiba Ceramic MFG. Co,. Ltd., composed of $Al_2O_3 > 99.5$ wt%, $SiO_2 < 0.10$ wt%, $Fe_2O_3 < 0.05$ wt%, $Na_2O < 0.10$ wt%, Cr < 2 ppm, Cd < 1 ppm, Pb < 1 ppm, and Hg < 1 ppm, was used. The bulk density of the plates was 3.7 g·cm^{-3}. The dimensions used for the glow curve measurements were $10 \times 10 \times 1$ mm^3. The Cr_2O_3 concentration in this study ranged from 0.01 to 1.0 wt%. In the demonstration of the verification of the RT plan, Cr-doped Al_2O_3 ceramic plates of $80 \times 80 \times 0.7$ mm^3 size were used (Fig. 1).

Figure 2 shows our glow curve measurement system and schematic diagram. The glow curves were recorded from room temperature up to 400 °C at a heating rate of 0.1 °C s^{-1} in
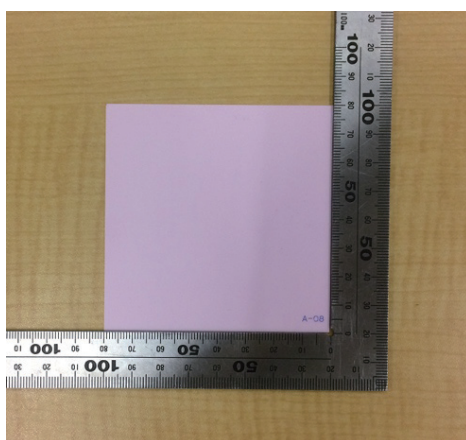

Fig. 1. (Color online) Low-melting-point Cr-doped Al_2O_3 ceramic plate ($80 \times 80 \times 0.7$ mm^3).
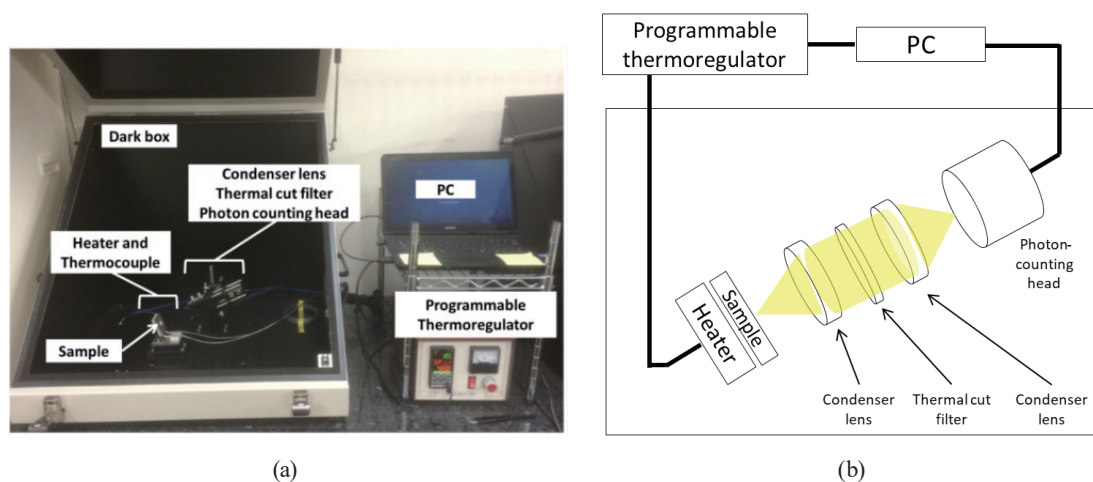
Fig. 2.   (Color online) Glow curve measurement system and schematic diagram.[8]

air. The sampling time was 10 s. The temperature was controlled using a Sakaguchi E.H VOC Corp. SCR-SHQ-A programmable thermoregulator. A Hamamatsu H11890-210 photon-counting head light detector was used to detect luminescence. The spectral sensitivity region of this photon counting was 400–700 nm. A thermal-cut filter was the only spectroscopic attachment used. The transmission band of the filter was 365–700 nm. The guaranteed spectral value of 700 nm was 0.43. The X-ray irradiation was carried out using a Varian CLINAC-21EX linear accelerator at 6 MV. The TL samples and a Scanditronix CC13 ion chamber were sandwiched between two tough-water phantoms (Kyoto Kagaku Co., Ltd) at a depth of 10 cm. The distance from the X-ray source to the chamber was 100 cm. The X-ray exposure dose was 5 Gy. In the dose-response curve measurements, the doses were 0.5–100 Gy.

The TL spectroscopic analysis was performed using a Hamamatsu PMA-11 multichannel CCD detector. The measurement system converted the photon-counting head shown in Fig. 2 into the multichannel CCD detector. The measured temperatures in the region ranged from room temperature to 350 °C. Rigaku Corp. Thermo plus EVO2 was used to measure the differential thermal analysis (DTA) and thermogravimetric analysis (TGA) curves.

2.2   TL imaging (2D) measurements

The TL imaging measurement system (Seisei Manufactory Co., Ltd.) consists of a complementary metal oxide semiconductor (CMOS) camera (ORCA®-Flash4.0 V2, C11440 -22CU), an 80×80 mm^2 heater (Sakaguchi E.H VOC Corp.), and a dark box (Fig. 3). After exposure, the door of the dark box was closed once the ceramic plates were set on the three pins. Next, the in-house-developed plate heater was raised to the top of the pins and then heated to 400 °C for 5 min. The heating rate was controlled using a programmable temperature controller, and the heater provided a flat temperature distribution and maintained the temperature ($<\pm3\%$). The TL images were captured using a CMOS camera equipped with a thermal cut filter.
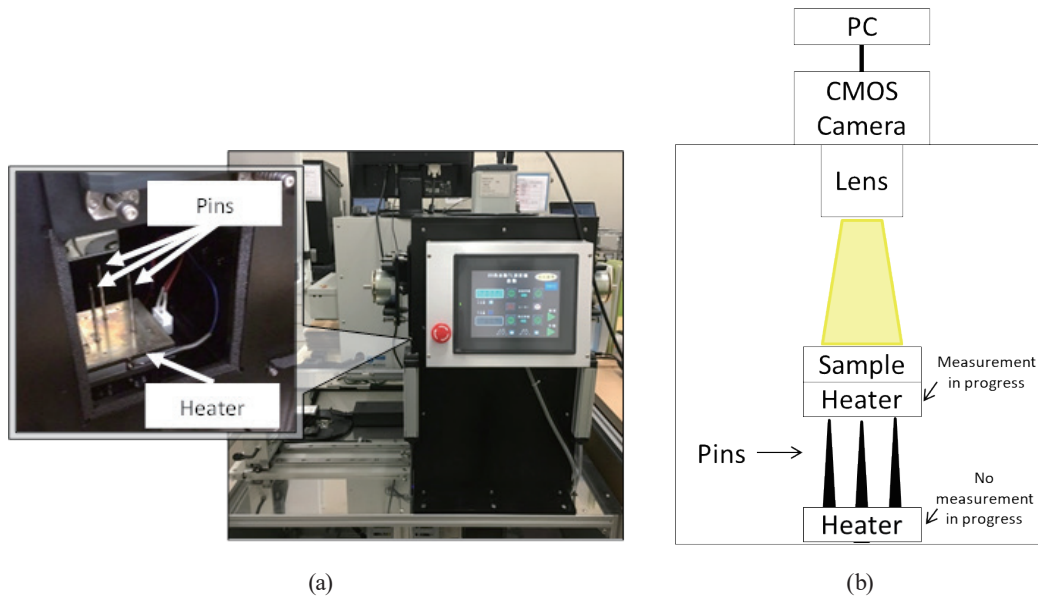
Fig. 3.   (Color online) (a) TL imaging (2D) measurement system and (b) schematic diagram.

3.   Results and Discussion

3.1   Basic TL characteristics

Figure 4 shows the TL intensity as a function of Cr_2O_3 concentration in Al_2O_3. The TL intensity increased accordingly as Cr was doped up to 0.05 wt%, then decreased. The highest sensitivity was about 4.8 times higher than that of nondoped Al_2O_3 at 0.05 wt% Cr doping.

Figure 5 shows TL glow curves of nondoped Al_2O_3 and 0–1.0 wt% Cr-doped Al_2O_3. The main glow peaks were located at about 150 °C for nondoped Al_2O_3. The glow peak at 300 °C was produced by the Cr-doped Al_2O_3, and the glow peak intensity gradually increased in relation to the Cr doping concentration until 0.05 wt%. From this point, it was suggested that the stabilization of a trap state was due to Cr doping. That is, we successfully improved its fading property dramatically. From similar observations,[9] the TL wavelength was 693 nm and was attributed to the ^2E–$^4A_2$ transition of the embedded Cr^{3+} (Fig. 6). In addition to the peak, a broad peak in the region of 600–800 nm was observed. We consider that the broad peak is TL-scattered by thermal vibration. That is, the peak was caused by stoke and antistoke lines. The glow peak temperature and TL intensity were changed by Cr doping; however, the TL wavelength did not depend on it.

In the dose-response curve measurements (Fig. 7), the Cr-doped Al_2O_3 had a high TL linearity from 0.5 to 10 Gy. Above 10 Gy, its TL efficiency showed supralinearity. Then, above 80 Gy, its measurement error increased.

Figure 8 shows the TL glow curve of 0.05 wt% Cr-doped Al_2O_3 phosphor after high-dose (150 Gy) X-ray irradiation. The TL glow curve did not change. That is, the TL characteristics of the Cr-doped Al_2O_3 phosphor have a high radiation resistivity.
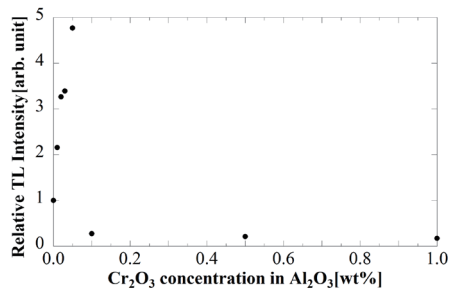
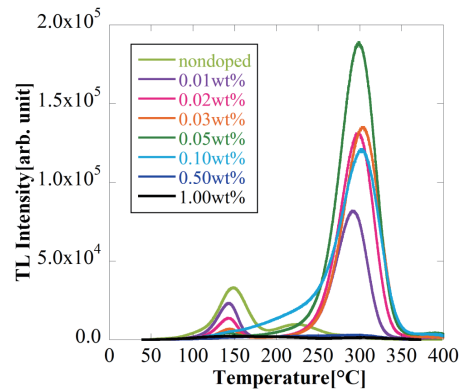Fig. 4.　Relative TL intensity as a function of Cr_2O_3 concentration in Al_2O_3.

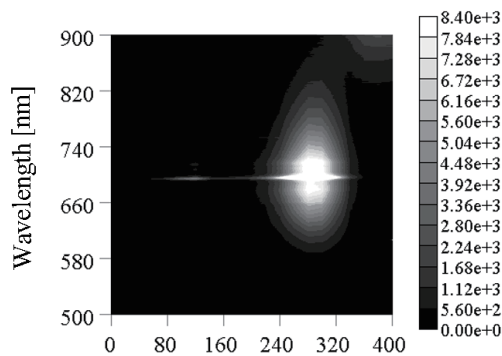Fig. 5.　(Color) TL glow curves of nondoped and Cr-doped Al_2O_3.

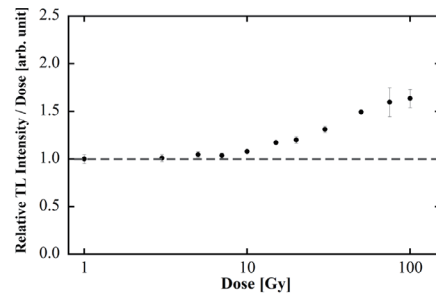Fig. 6.　TL spectra of 0.05 wt% Cr-doped Al_2O_3.

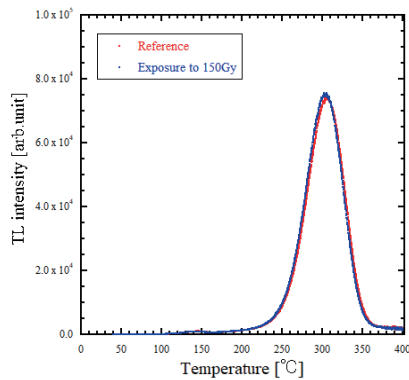Fig. 7.　Dose-response curve of 0.05 wt% Cr-doped Al_2O_3.

Fig. 8.　(Color) TL glow curve of 0.05 wt% Cr-doped Al_2O_3 phosphor after high-dose (150 Gy) X-ray irradiation.

Table 1
Reproducibility of relative TL intensity of 0.05 wt% Cr-doped Al_2O_3 (annealed at 500 ℃).

	Relative TL intensity
1st	2.63×10^8
2nd	2.65×10^8
3rd	2.68×10^8
CV (%)	0.93

　　Table 1 shows the reproducibility of the relative TL intensity of the 0.05 wt% Cr-doped Al_2O_3 (annealed at 500 ℃). It had a high reproducibility with a coefficient variation (CV) of <1.0%.

　　In the reproducibility of the DTA and TGA curves, the results did not depend on the 25 identical thermal cycles from room temperature to 1000 ℃. It was indicated that the 0.05 wt% Cr-doped Al_2O_3 has high thermal stability.

3.2   Demonstration of vilification of RT plan

RT planning is made using CT images.   A 0.05 wt% Cr-doped Al_2O_3 plate stacked in a tough-water phantom was CT-scanned. The CT images were forwarded to a treatment planning system (TPS) (Varian medical systems, Eclipse, Ver. 13.6) and two types of dose distribution were made using a linear accelerator (Varian medical systems, Clinac iX) with a 10 MV photon beam. The field sizes were 5×5 cm^2 in static irradiation [Fig. 9(a)] and 4×5 cm^2 in arc irradiation [Fig. 9(b)]. The gantry was rotated counterclockwise from 140 to 240 degrees in the arc.

Figure 10 shows the dose distribution measured using a 0.05 wt% Cr-doped Al_2O_3 plate subjected to static irradiation. The dose profile obtained using the Al_2O_3 plate (red line) is compared with that obtained using TPS. Figure 11 shows the OCR curve of the 0.05 wt% Cr-doped Al_2O_3 plate and TPS. The OCRs of the 0.05 wt% Cr-doped Al_2O_3 plate and TPS were in agreement within 1.5%.

Figure 12 shows the dose distribution measured using the 0.05 wt% Cr-doped Al_2O_3 plate in arc irradiation. Figure 13 shows the OCR curve of the 0.05 wt% Cr-doped Al_2O_3 plate and TPS. The OCRs of the 0.05 wt% Cr-doped Al_2O_3 plate and TPS were in agreement within 1.0%.
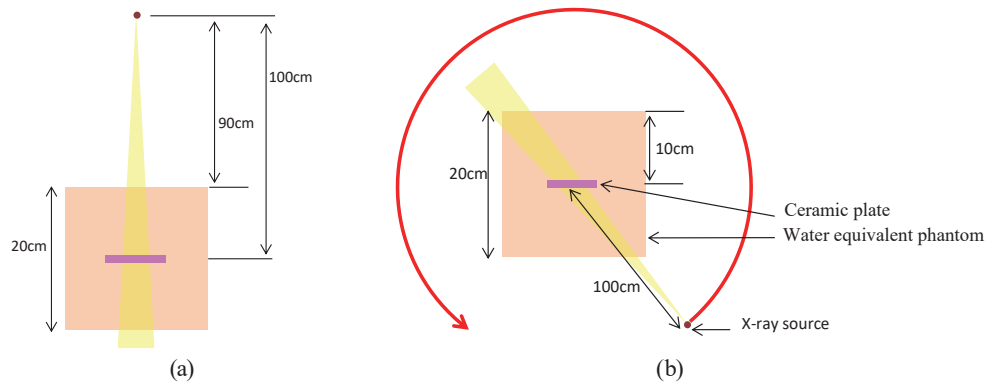

Fig. 9.   (Color) Measurement alignment: (a) static irradiation and (b) arc irradiation.
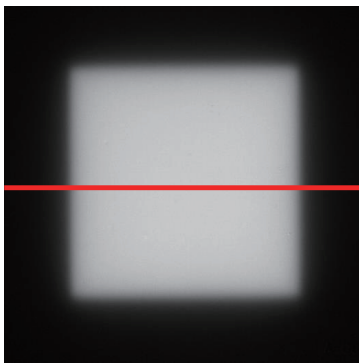

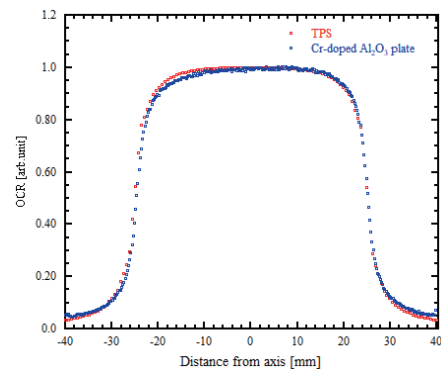Fig. 10. (Color) Dose distribution of 0.05 wt% Cr-doped Al_2O_3 plate subjected to static irradiation.

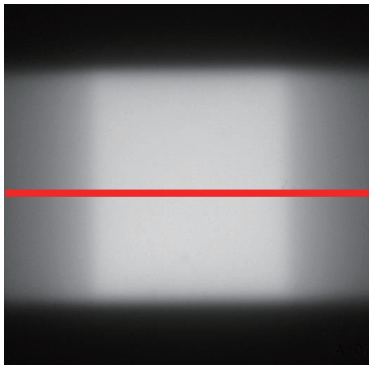Fig. 11.   (Color) OCR curve of static irradiation.

Fig. 12. (Color) Dose distribution of 0.05 wt% Cr-doped Al_2O_3 plate subjected to arc irradiation.
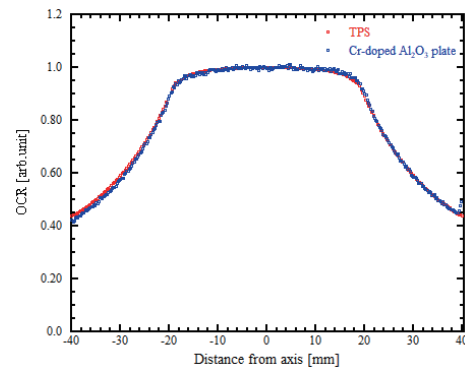

Fig. 13. (Color) OCR curve of arc irradiation.

4. Conclusions

We investigated the basic TL characteristics of Cr-doped low-melting-point Al_2O_3. The Cr_2O_3 concentration in this study ranged from 0.01 to 1.0 wt%. Owing to the stabilization of the trapped state caused by Cr doping, we successfully improved the low-melting-point Al_2O_3 fading property dramatically. Then, the sensitivity of 0.05 wt% Cr-doped Al_2O_3 to X-rays was about 4.8 times higher than that of nondoped Al_2O_3, allowing the Al_2O_3 to maintain its attractive properties to X-rays. Furthermore, the 0.05 wt% Cr-doped Al_2O_3 had good properties for dosimetry owing to its high TL sensitivity, high reproducibility, high radiation resistivity, and high thermal stability in two dimensions. Finally, we demonstrated 2D verifications of RT plans using Cr-doped Al_2O_3 ceramic plates. The results were in good agreement with RT plans. We will attempt the 2D dose distribution of a large area of approximately 150×150 mm^2 using TL plates with this material soon.

References

1   D. Kabat, D. Nahajowski, E. Góra, B. Rozwadowska-Bogusz, J. Lesiak, B. Polak, Ł. Czopyk, P. Olko, and M. P. R. Waligórski: Radiat. Meas. **43** (2008) 1004.
2   K. Kisielewicz, J. Świebocka, Ł. Czopyk, M. Kłosowski, J. Lesiak, E. Byrski, D. Kabat, M. Wawrzak, A. Śladowska, A. Dziecichowicz, P. Olko, and M. P. R.Waligórski: Radiat. Meas. **45** (2010) 716.
3   L. Marrazzo, S. Pallotta, M. Kłosowski, Ł. Czopyk, M. Bucciolini, P. Olko, and M. P. R. Waligórski: Radiat. Meas. **51–52** (2013) 25.
4   K. Shinsho, Y. Tomizawa, H. Horikawa, S. Miyajima, H. Saitoh, and A. Urushiyama: Radiat. Meas. **46** (2011) 1912.
5   K. Shinsho, Y. Koba, G. Wakabayashi, S. Tamatsu, S. Fukuda, R. Morimoto, D. Maruyama, H. Saitoh, and N. Sakurai: Radiat. Meas. **62** (2014) 15.

6 S. Yanagisawa, K. Shinsho, M. Inoue, Y. Koba, K. Matsumoto, H. Ushiba, and T. Andoh: Radiat. Meas. **106** (2017) 326.
7 D. Lapraz, P. Lacconi, D. Daviller, and B. Guilhot: Phys. Status Solidi A **126** (1991) 521.
8 K. Shinsho, Y. Kawaji, S. Yanagisawa, K. Otsubo, Y. Koba, G. Wakabayashi, K. Matsumoto, and H. Ushiba: Appl. Radiat. Isot. **111** (2016) 117.
9 G. P. Summers: Radiat. Prot. Dosim. **8** (1984) 69.